

**Chapter 3:**  
**Comparison of Incoherent and Coherent Yields of**  
**DNA-mediated Charge Transport<sup>§</sup>**

---

<sup>§</sup> This work was performed in collaboration with Ms. Stephanie Wuerth.

### 3.1. INTRODUCTION

Molecular charge transport (CT) has been subject to extensive theoretical and experimental studies,<sup>1-4</sup> since nanoscale device elements provide both novel sensing platforms and the potential to extend Moore's Law beyond the current limits of solid-state lithography. The properties of individual assemblies can be difficult to predict, however, because the mechanism of CT can change as a result of small variations in donor and bridge energies, bridge length, or environmental factors. A transition from exponential to geometric distance dependence is frequently interpreted as being due to a change in the dominant mechanism from coherent superexchange over short bridges to incoherent hopping over long bridges. In fact, it is assumed that fast, coherent CT over long distances is impossible, as a bridge low enough in potential to mediate long-range superexchange will be rapidly occupied by charge itself, and that incoherent CT will then dominate.<sup>5</sup> Given these conditions, it is not surprising that a variety of bridging systems have been found to transition between superexchange and hopping for increasing bridge length and decreasing separation of bridge and donor energy levels.<sup>6-7</sup>

DNA has been extensively studied as a molecular bridge, due to the synthetic accessibility of diverse, well-defined structures,<sup>8,9</sup> the biotechnological applications of DNA sensors,<sup>10,11</sup> and the relevance of DNA-mediated charge migration to biological function.<sup>12</sup> DNA CT is mediated by the  $\pi$ -stack of the base pairs, and for well-coupled donors and acceptors, can lead to charge migration over 200 Å.<sup>13</sup> Importantly, fluorescence quenching by CT through DNA has been observed for donor-acceptor separations of up to eight base pairs, indicating that single-step CT can occur over long distances as well.<sup>14</sup> For the quenching of the fluorescent adenine analogue 2-aminopurine

(Ap) by guanine across an adenine tract, the distance dependence is shallow and periodic. The periodicity has been assigned as a consequence of transient delocalization over 3 to 4 base pairs being ideal for forming a CT-active state<sup>14</sup>; this delocalization length has also been found from other experimental and theoretical studies.<sup>15-17</sup> Furthermore, these CT-active states are non-equilibrium states, and their formation is conformationally gated.<sup>14,18,19</sup>

Another approach for studying DNA CT is to measure the decomposition yields of the bases themselves, with guanine being the most reactive to oxidative damage.<sup>20-22</sup> Because guanine radical decomposition is slow in the absence of additional reactive species, such as superoxide,<sup>23</sup> this measure is convoluted with the trapping rate.<sup>21</sup> We have recently studied CT yield using fast *N*-cyclopropyl radical traps,<sup>24</sup> as substituents on guanine,<sup>19,25</sup> adenine,<sup>26</sup> and cytosine<sup>17</sup> through the exocyclic amines. *N*<sub>2</sub>-cyclopropylguanine, incorporated into DNA, is readily decomposed by photoexcited thionine, despite the femtosecond recombination that has been measured between guanine radical cation and thionine radical anion, indicating the power of these subnanosecond traps for measuring pre-equilibrium hole occupation.<sup>19,22,25</sup>

By using fast radical traps at the hole acceptor, we can determine the yield of total CT. Herein, we measure the quantum yields of total CT in comparable assemblies containing Ap and <sup>CP</sup>G separated by adenine tracts. Single-step CT yield is derived from previous measurements of steady-state fluorescence quenching.<sup>14</sup> By comparing the yields of total and single-step CT, we can see the relative contributions of coherent and incoherent channels.

## 3.2. METHODS

### 3.2.1. OLIGONUCLEOTIDE SYNTHESIS.

DNA oligonucleotides were synthesized trityl-on using standard phosphoramidite chemistry on an ABI DNA synthesizer with Glen Research reagents. 2-aminopurine (Ap) was incorporated as the *N*<sub>2</sub>-dimethylaminomethylidene protected phosphoramidite (Glen Research). <sup>CP</sup>G-modified oligonucleotides were prepared by incorporating the precursor base, 2-fluoro-*O*<sub>6</sub>-paraphenylethyl-2'-deoxyinosine (Glen Research), as a phosphoramidite at the desired position. The resin was then reacted with 1 M diaza(1,3)bicyclo[5.4.0]undecane (DBU, Aldrich) in acetonitrile to effectively remove the *O*<sub>6</sub> protecting group. Similarly, <sup>CP</sup>A-modified oligonucleotides were prepared by incorporating the precursor base, *O*<sub>6</sub>-phenylinosine (Glen Research) as a phosphoramidite at the desired position. For both <sup>CP</sup>G- and <sup>CP</sup>A- containing strands, the oligonucleotides were subsequently incubated overnight in 6 M aqueous cyclopropylamine (Aldrich) at 60 °C resulting in substitution, base deprotection, and simultaneous cleavage from the resin. The cleaved strands were dried *in vacuo* and purified by reversed-phase HPLC, detritylated by 80% acetic acid for 15 min, and repurified by reversed-phase HPLC. Oligonucleotides were characterized by MALDI-TOF mass spectrometry. Sequences are provided in **Table 3.1**.

All oligonucleotides were suspended in a buffer containing 50 mM NaCl, 5 mM sodium phosphate, pH 7 and quantified using UV-visible spectroscopy. Duplexes were prepared by heating equal concentrations of complementary strands to 90 °C for 5 min and slow cooling to ambient temperature.

**Table 3.1. DNA assemblies for oxidative decomposition experiments**

Ap-A <sub>0</sub> - <sup>CP</sup> G	5'-GATTATAGACATATTI <b>Ap</b> - <sup>CP</sup> <b>G</b> ITATTAAGTACATTAC-3' 3'-CTAATATCTGTATAACT - CCATAATTCATGTAATG-5'
Ap-A <sub>1</sub> - <sup>CP</sup> G	5'-GATTATAGACATATTI <b>Ap-A</b> - <sup>CP</sup> <b>G</b> ITATTAAGTACATTAC-3' 3'-CTAATATCTGTATAACT - <b>T</b> - CCATAATTCATGTAATG-5'
Ap-A <sub>2</sub> - <sup>CP</sup> G	5'-GATTATAGACATATTI <b>Ap-AA</b> - <sup>CP</sup> <b>G</b> ITATTAAGTACATTAC-3' 3'-CTAATATCTGTATAACT - <b>TT</b> - CCATAATTCATGTAATG-5'
Ap-A <sub>3</sub> - <sup>CP</sup> G	5'-GATTATAGACATATTI <b>Ap-AAA</b> - <sup>CP</sup> <b>G</b> ITATTAAGTACATTAC-3' 3'-CTAATATCTGTATAACT - <b>TTT</b> - CCATAATTCATGTAATG-5'
Ap-A <sub>4</sub> - <sup>CP</sup> G	5'-GATTATAGACATATTI <b>Ap-AAAA</b> - <sup>CP</sup> <b>G</b> ITATTAAGTACATTAC-3' 3'-CTAATATCTGTATAACT - <b>TTTT</b> - CCATAATTCATGTAATG-5'
Ap-A <sub>5</sub> - <sup>CP</sup> G	5'-GATTATAGACATATTI <b>Ap-AAAAA</b> - <sup>CP</sup> <b>G</b> ITATTAAGTACATTAC-3' 3'-CTAATATCTGTATAACT - <b>TTTTT</b> - CCATAATTCATGTAATG-5'
Ap-A <sub>6</sub> - <sup>CP</sup> G	5'-GATTATAGACATATTI <b>Ap-AAAAAA</b> - <sup>CP</sup> <b>G</b> ITATTAAGTACATTAC-3' 3'-CTAATATCTGTATAACT - <b>TTTTTT</b> - CCATAATTCATGTAATG-5'
Ap-A <sub>7</sub> - <sup>CP</sup> G	5'-GATTATAGACATATTI <b>Ap-AAAAAAA</b> - <sup>CP</sup> <b>G</b> ITATTAAGTACATTAC-3' 3'-CTAATATCTGTATAACT - <b>TTTTTTT</b> - CCATAATTCATGTAATG-5'
Ap-A <sub>8</sub> - <sup>CP</sup> G	5'-GATTATAGACATATTI <b>Ap-AAAAA AAA</b> - <sup>CP</sup> <b>G</b> ITATTAAGTACATTAC-3' 3'-CTAATATCTGTATAACT - <b>TTTTTTTT</b> - CCATAATTCATGTAATG-5'
Ap-A <sub>9</sub> - <sup>CP</sup> G	5'-GATTATAGACATATTI <b>Ap-AAAAA AAAA</b> - <sup>CP</sup> <b>G</b> ITATTAAGTACATTAC-3' 3'-CTAATATCTGTATAACT - <b>TTTTTTTTT</b> - CCATAATTCATGTAATG-5'
Ap-A <sub>11</sub> - <sup>CP</sup> G	5'-GATTATAGACATATTI <b>Ap-AAAAA AAAA A</b> - <sup>CP</sup> <b>G</b> ITATTAAGTACATTAC-3' 3'-CTAATATCTGTATAACT - <b>TTTTTTTTTTTT</b> - CCATAATTCATGTAATG-5'
Ap-A <sub>12</sub> - <sup>CP</sup> G	5'-GATTATAGACATATTI <b>Ap-AAAAA AAAA A A</b> - <sup>CP</sup> <b>G</b> ITATTAAGTACATTAC-3' 3'-CTAATATCTGTATAACT - <b>TTTTTTTTTTTTT</b> - CCATAATTCATGTAATG-5'
Ap-A <sub>7</sub> - <sup>CP</sup> A <sup>4</sup>	5'-GATTATAGACATATTI <b>Ap-AAA</b> <sup>CP</sup> <b>AAAA</b> -ITATTAAGTACATTAC-3' 3'-CTAATATCTGTATAACT - <b>TTT TTT</b> -CATAATTCATGTAATG-5'
Ap-A <sub>7</sub> - <sup>CP</sup> A <sup>7</sup>	5'-GATTATAGACATATTI <b>Ap-AAAAA</b> <sup>CP</sup> <b>A</b> -ITATTAAGTACATTAC-3' 3'-CTAATATCTGTATAACT - <b>TTTTTT T</b> -CATAATTCATGTAATG-5'
LC-A <sub>7</sub> - <sup>CP</sup> A <sup>7</sup>	5'-GATTATAGACATATTI <b>A-AAAAA</b> <sup>CP</sup> <b>A</b> -ITATTAAGTACATTAC-3' 3'-CTAATATCTGTATAACT- <b>TTTTTT T</b> -CATAATTCATGTAATG-5'
Ap-A <sub>5</sub> - <sup>CP</sup> A <sup>3</sup>	5'-GATTATAGACATATTI <b>Ap-AA</b> <sup>CP</sup> <b>AAA</b> -IITATTAAGTACATTAC-3' 3'-CTAATATCTGTATAACT - <b>TT TTT</b> -CCATAATTCATGTAATG-5'



### 3.2.2. PHOTOOXIDATION EXPERIMENTS

Samples were irradiated at ambient temperature. Duplexes (30 mL, 10 mM) in PBS were irradiated on a 1000 W Hg/Xe lamp equipped with a monochromator at 325 nm for 30 sec unless otherwise indicated. To analyze for <sup>CP</sup>A or <sup>CP</sup>G decomposition following irradiation, samples were digested to the component nucleosides by phosphodiesterase I (USB) and alkaline phosphatase (Roche) to completion. The resulting deoxynucleosides were analyzed by reversed-phase HPLC using a Chemcobond 5-ODS-H, 4.6 mm × 100 mm column. The amount of <sup>CP</sup>G or <sup>CP</sup>A per duplex was determined by taking the ratio of the area of the HPLC peak for d<sup>CP</sup>G or d<sup>CP</sup>A to the area of the peak for dT, the internal reference. The decomposition yield is taken as the percent loss of <sup>CP</sup>G or <sup>CP</sup>A between an irradiated sample and the dark control; at least nine samples and three dark controls are performed for each sequence. Dark control HPLC traces were quantified for the relative amounts of dA, dC, dG, dI, dT, d<sup>CP</sup>A and d<sup>CP</sup>G based on duplex sequence, to confirm strand stoichiometry. Actinometry was performed using a 6 mM ferrioxalate standard.<sup>27</sup> The given quantum yield is for the efficiency from the Ap\* state to the ring-opened product. Errors are presented at 90% standard error of the mean, using the Student's t-distribution at the appropriate degrees of freedom to determine confidence intervals.

## 3.3. RESULTS AND DISCUSSION

### 3.3.1. EXPERIMENTAL DESIGN

To determine the quantum yield of guanine oxidation by photoexcited 2-aminopurine (Ap), we constructed a series of duplex assemblies with Ap separated

from  ${}^{\text{CP}}\text{G}$  by adenine tracts of varying length, and measured the decomposition of the radical trap upon irradiation. Inosines are used as barriers for CT from  $\text{Ap}^*$  to bases outside of the tract; the high-potential inosine serves as a tunneling barrier, preventing depopulation of the aminopurine excited state by nucleotides outside of the bridge.<sup>28</sup> Because  ${}^{\text{CP}}\text{G}$  is a fast radical trap, its decomposition yield represents the total yield of all pathways that lead to oxidation of guanine, as long as back electron transfer is slower than ring-opening. Importantly, in this work we have determined quantum yields for  $\text{Ap}-(\text{A})_n-{}^{\text{CP}}\text{G}$  duplexes that are identical to sequences for which single-step CT yields have been determined,<sup>14</sup> allowing us to compare the relative yields of single-step and multi-step CT (**Figure 3.1**). For direct comparison of guanine and adenine oxidation, we also constructed assemblies containing the  ${}^{\text{CP}}\text{A}$  radical trap at various positions along the bridge. We use  $\text{Ap}-\text{A}_n-{}^{\text{CP}}\text{A}^m-\text{Y}$  to indicate a sequence with an adenine tract of length  $n$ , a  ${}^{\text{CP}}\text{A}$  at position  $m$  along the tract, and terminal base  $Y$  at the end of the tract ( $Y = \text{G}, \text{I},$  or  ${}^{\text{CP}}\text{G}$ ). All eight nucleosides are well resolved by HPLC, allowing straightforward quantification of the  ${}^{\text{CP}}\text{G}$  or  ${}^{\text{CP}}\text{A}$  content per duplex.

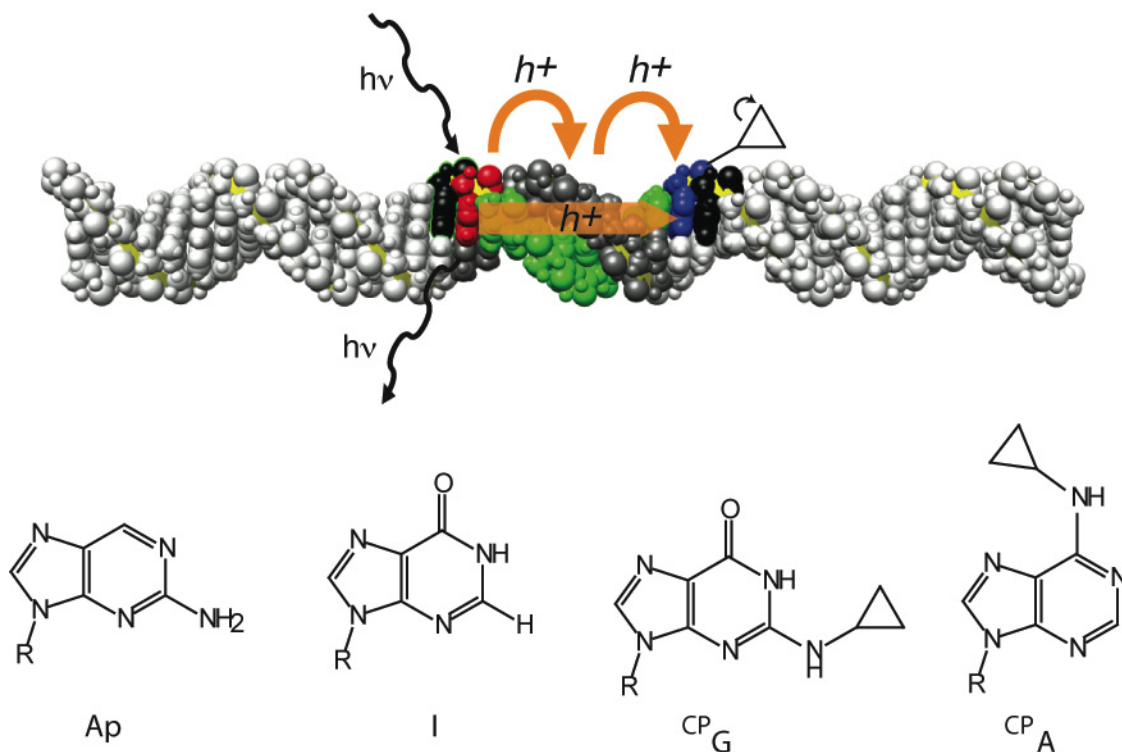


**Figure 3.1.** Pathways for single-step and multi-step CT in this work. 2-aminopurine (Ap) is selectively excited, and relaxes to a ground excited state that is competent for oxidizing guanine (blue) through the adenine bridge or oxidizing adenine (green) directly. A hole on adenine can then hop to the guanine. These CT processes are in competition with emission; hence emission yield is attenuated by charge transport. Structures of the four unnatural bases employed are provided.

### 3.3.2. DNA-MEDIATED OXIDATIVE DECOMPOSITION OF ${}^{\text{CP}}\text{G}$ BY $\text{Ap}^*$

Upon irradiation, facile decomposition is observed for  ${}^{\text{CP}}\text{G}$ , indicating oxidation of the guanine by photoexcited Ap (**Table 3.2**). For short donor-acceptor separation ( $n = 0-3$ ), little ring-opening occurs, because charge recombination between the aminopurine radical anion and guanine cation radical is competitive with radical trapping at the  ${}^{\text{CP}}\text{G}$ .<sup>19,25</sup> For four intervening adenines, the quantum yield peaks at about 1%, followed by a slow decay for longer sequences. The peak value is comparable to the quantum yield (1.7%) of emission from Ap-(A)<sub>n</sub>-I sequences,<sup>14</sup> and the profile is similar to that which has previously been observed for oxidation of  ${}^{\text{CP}}\text{G}$  by Ap.<sup>19</sup>

### 3.3.3. DETERMINATION OF SINGLE-STEP CT YIELDS FROM FLUORESCENCE QUENCHING YIELDS

Our values of single-step CT yield come from steady-state fluorescence quenching experiments with Ap.<sup>19,29</sup> The fluorescence of Ap in DNA is strongly quenched versus the free nucleoside, even if there is no guanine in the assembly. The presence of a nearby guanine leads to further quenching of fluorescence by a CT mechanism.<sup>29-32</sup> Adenine oxidation by  $\text{Ap}^*$ , while favorable, is far slower than guanine oxidation, as is reduction of cytosine and thymidine by  $\text{Ap}^*$ .<sup>32,33</sup> If the CT quenching by guanine competed with all other relaxation mechanisms, this would imply near quantitative CT between photoexcited Ap and guanine, inconsistent with transient absorption spectroscopy studies on the Ap excited state that find the decays of photoexcited Ap(A)<sub>3</sub>I and Ap(A)<sub>3</sub>G in duplex DNA to be indistinguishable,<sup>32</sup> and with

**Table 3.2. Quantum yields of decomposition for CP-modified bases**

Sequence	Quantum Yield of Decomposition
Ap-A <sub>0</sub> - <sup>CP</sup> G	0.00008 ± 0.00010 <sup>a</sup>
Ap-A <sub>1</sub> - <sup>CP</sup> G	0.00002 ± 0.00008
Ap-A <sub>2</sub> - <sup>CP</sup> G	0.00029 ± 0.00016
Ap-A <sub>3</sub> - <sup>CP</sup> G	0.00344 ± 0.00009
Ap-A <sub>4</sub> - <sup>CP</sup> G	0.0086 ± 0.0002
Ap-A <sub>5</sub> - <sup>CP</sup> G	0.0068 ± 0.0005
Ap-A <sub>6</sub> - <sup>CP</sup> G	0.0026 ± 0.0005
Ap-A <sub>7</sub> - <sup>CP</sup> G	0.0017 ± 0.0003
Ap-A <sub>8</sub> - <sup>CP</sup> G	0.00099 ± 0.00003
Ap-A <sub>9</sub> - <sup>CP</sup> G	0.0013 ± 0.0001
Ap-A <sub>11</sub> - <sup>CP</sup> G	0.00049 ± 0.00006
Ap-A <sub>12</sub> - <sup>CP</sup> G	0.0007 ± 0.0001
Ap-A <sub>7</sub> - <sup>CP</sup> A <sup>4</sup>	0.0096
Ap-A <sub>7</sub> - <sup>CP</sup> A <sup>7</sup>	0.00096
LC-A <sub>7</sub> - <sup>CP</sup> A <sup>7</sup>	0.000066
Ap-A <sub>5</sub> - <sup>CP</sup> A <sup>3</sup>	0.0019 ± 0.0002
Ap-A <sub>5</sub> - <sup>CP</sup> A <sup>3</sup> -G	0.0020 ± 0.0002
Ap-A <sub>5</sub> - <sup>CP</sup> A <sup>3</sup> - <sup>CP</sup> G	0.0017 ± 0.0002 ( <sup>CP</sup> A)
Ap-A <sub>5</sub> - <sup>CP</sup> A <sup>3</sup> - <sup>CP</sup> G	0.0011 ± 0.0003 ( <sup>CP</sup> G)
Ap-A <sub>5</sub> - <sup>CP</sup> A <sup>2</sup>	0 ± 0.0002
Ap-A <sub>5</sub> - <sup>CP</sup> A <sup>4</sup>	0.0061 ± 0.0002
Ap-A <sub>5</sub> - <sup>CP</sup> A <sup>5</sup>	0.0021 ± 0.0002
Ap-A <sub>6</sub> - <sup>CP</sup> A <sup>3</sup>	0.0022 ± 0.0002
Ap-A <sub>6</sub> - <sup>CP</sup> A <sup>3</sup> -G	0.0020 ± 0.0001
Ap-A <sub>6</sub> - <sup>CP</sup> A <sup>3</sup> - <sup>CP</sup> G	0.0023 ± 0.0002 ( <sup>CP</sup> A)
Ap-A <sub>6</sub> - <sup>CP</sup> A <sup>3</sup> - <sup>CP</sup> G	0.0004 ± 0.0003 ( <sup>CP</sup> G)

a. Errors are reported as 90% s.e.m.

the relatively low overall quantum yield of  ${}^{\text{CP}}\text{G}$  decomposition. Recent measurements of the time-resolved fluorescence and transient absorption of aminopurine constructs have determined that the hot excited state of aminopurine is quenched prior to vibrational relaxation ( $\leq 200$  fs).<sup>34</sup> This was ascribed to direct CT, but might also involve stacking interactions allowing barrierless conversion to the dark  $n\pi^*$  state,<sup>35</sup> which is only 0.4 eV above the relaxed  $\pi\pi^*$  state.<sup>36</sup> Furthermore, the temperature dependence of the  $\text{Ap}^*$  picosecond decay components supports the presence of two different populations of assemblies. Those in an initially CT-active state proceed to rapid CT, while CT for those in a less active configuration is conformationally gated.<sup>37</sup> This explains the similar picosecond decay kinetics of photoexcited  $\text{Ap}(\text{A})_3\text{I}$  and  $\text{Ap}(\text{A})_3\text{G}$  despite the difference in steady-state fluorescence quenching; the populations undergoing CT may not be in direct competition.

In summary, it appears that CT from  $\text{Ap}^*$  to guanine for assemblies that are initially in CT-active states competes only with emission. If single-step CT to guanine is in competition with other relaxation mechanisms as well, then this model will underestimate the quantum yield. For the above description of the excited state dynamics (**Figure 3.2**), the quantum yield of CT from the relaxed, CT-active state corresponds to the difference in emission quantum yields between assemblies that contain redox-active guanine and those that contain redox-inactive inosine. We can compare these values to our measurements for total CT yield from  ${}^{\text{CP}}\text{G}$  decomposition.

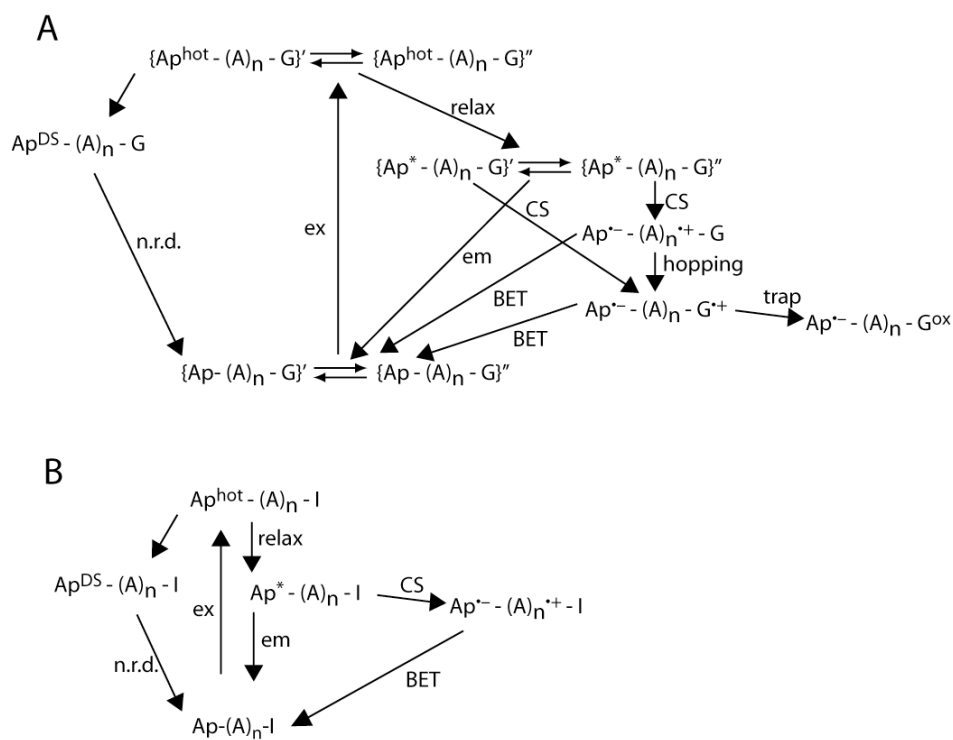


**Figure 3.2.** Excited-state dynamics of aminopurine in DNA. All duplexes are initially excited (ex) to a hot state ( $\text{Ap}^{\text{hot}}$ ), which can either decay through a non-radiative pathway (n.r.d.) through a dark state (DS), or relax to the persistent excited state ( $\text{Ap}^*$ ). For guanine-containing duplexes (**A**), some assemblies are in a CT-active state with respect to guanine at the time of excitation (single prime), while others are not (double prime). Assemblies that are not in a CT-active state with respect to guanine, or that contain inosine instead of guanine (**B**), can undergo either emission (em) or charge separation (CS) to generate the adenine cation radical, which regenerates the ground state upon back electron transfer (BET). If a guanine is present, the hole on adenine can hop to guanine. Assemblies that are in a CT-active state with respect to guanine can undergo either emission or charge separation to guanine. Guanine cation radical then decays by either ring-opening (in the  $^{\text{CP}}\text{G}$  constructs) or BET. Relative heights are arbitrary.

### 3.3.4. COMPARISON OF SINGLE-STEP AND TOTAL CT YIELDS

It is not surprising that most CT in photoexcited Ap-A<sub>n</sub>-<sup>CP</sup>G is multi-step for  $n = 4-6$  (**Figure 3.3**). Aminopurine is competent to oxidize adenine directly, generating a hole that can migrate across the adenine tract to guanine. Unexpectedly, the distance dependence for the total CT is steeper than the coherent component, such that all CT is coherent for  $n = 7, 8$ . This represents the first case of coherent CT overtaking incoherent CT at longer distances.

Furthermore, the changing contributions of the two mechanisms could not have been determined by solely measuring the total CT yield. The distance dependence for  $n > 4$  is fit equally well by geometric or exponential decay (**Figure 3.4**); generally, fits of CT rates to these two decays tend to be equivalent for realistic bridge lengths.<sup>38</sup> In fact, the distance dependence of the total yield is similar to that observed for total CT between stilbenes in photoexcited stilbene-capped DNA hairpins, which are incompetent for coherent CT over more than a couple of base pairs.<sup>39</sup> The geometric dependence gives an  $\eta$  of 2.6, corresponding to a small bias towards migration away from the <sup>CP</sup>G,<sup>40</sup> probably due to coulombic attraction to the aminopurine anion radical.<sup>41</sup>

The yields of coherent CT determined using the model of **Figure 3.2** are the least generous possible, i.e. CT to guanine is only in competition with emission. If CT to guanine competes with CT to adenine, or with the pre-relaxation dynamics, then the coherent CT yield is necessarily higher than the values we use for the analysis here. Similarly, if charge injection from the hot aminopurine state can lead to ring-opening, our decomposition yield is an overestimate for the total CT yield from the relaxed excited

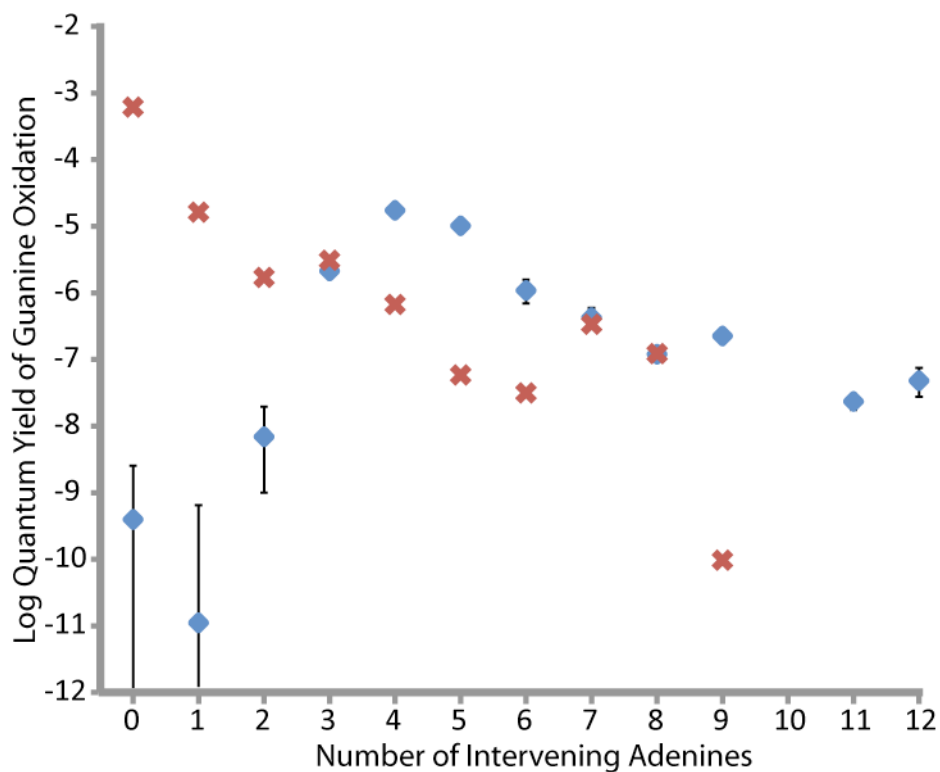


**Figure 3.3.** CT quantum yields as a function of bridge length for the Ap-A<sub>n</sub>-<sup>CP</sup>G series (blue diamonds), as determined by ring-opening of <sup>CP</sup>G, on a natural log scale. Duplexes (10 mM) were irradiated at ambient temperature for 30 sec at 325 nm in 5 mM sodium phosphate, 50 mM NaCl, pH 7.0 as described in the text. The experiments were repeated at least nine times, with the results averaged and the error expressed as 90% confidence intervals of the mean. On the same plot, fluorescence quenching quantum yields for the analogous duplexes are shown for comparison (red x's, data from reference 14).

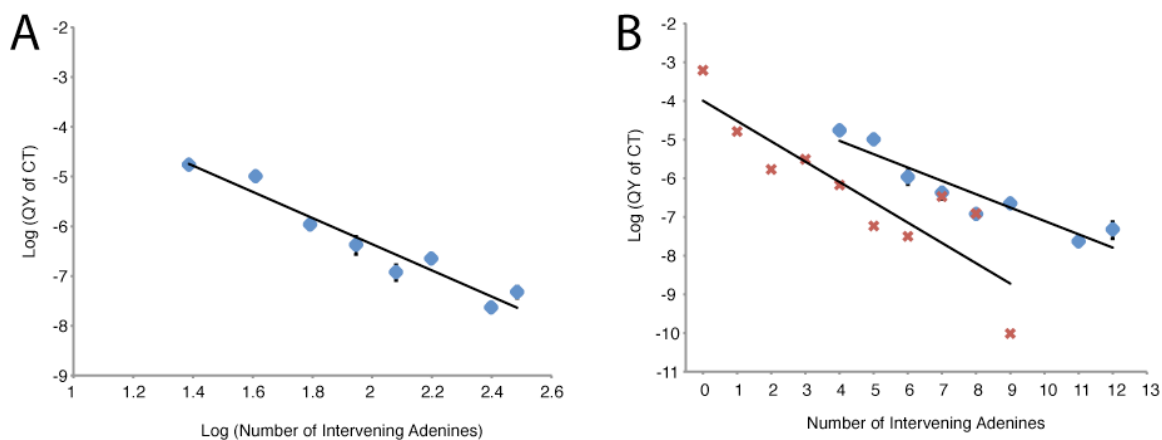


**Figure 3.4.** Fits of distance-dependent CT yields for the  $A_p-A_n\text{-}^{CP}G$  series on a log (A) and semilog (B) scale. Conditions are as in **Figure 3.3**. For the total CT yield (blue diamonds), the data is equally well-fit by geometric and exponential decay with distance. The decay constant from fitting to geometric decay,  $\eta$ , is 2.6. The decay constant from fitting to exponential decay is 0.3 per base ( $0.1 \text{ \AA}^{-1}$ ). The single-step CT yields (red x's) do not fit well to an exponential distance dependence, due to the periodicity.

state. Hence, our values for coherent yield are lower bounds, while our values for total yield are upper bounds. Total CT is necessarily greater than its coherent component. In this context, the equivalence of the CT yields for coherent and total transport at  $n = 7, 8$  validates the model for the excited-state dynamics.

### 3.3.5. DNA-MEDIATED OXIDATIVE DECOMPOSITION OF ${}^{\text{CP}}\text{A}$ BY $\text{Ap}^*$

To directly measure oxidation of the bridge, we inserted  ${}^{\text{CP}}\text{A}$ , an unnatural adenine analogue, into the adenine tract. The potential of  $\text{Ap}^*$  is barely adequate for adenine oxidation, but we find rapid decomposition of  ${}^{\text{CP}}\text{A}$  upon irradiation of Ap-containing duplexes (**Figure 3.5**). As  ${}^{\text{CP}}\text{A}$  is moved along the 5-adenine tract, there is the same initial increase in yield due to charge recombination competing with trapping (**Table 3.2**).

We would expect that  ${}^{\text{CP}}\text{A}$  in the adenine tract would interfere with incoherent oxidation of  ${}^{\text{CP}}\text{G}$ . Far less  ${}^{\text{CP}}\text{G}$  decomposition is observed for  $\text{Ap-A}_5\text{-}{}^{\text{CP}}\text{A}^3\text{-}{}^{\text{CP}}\text{G}$  and  $\text{Ap-A}_6\text{-}{}^{\text{CP}}\text{A}^3\text{-}{}^{\text{CP}}\text{G}$  than the respective assemblies without  ${}^{\text{CP}}\text{A}$ ,  $\text{Ap-A}_5\text{-}{}^{\text{CP}}\text{G}$  and  $\text{Ap-A}_6\text{-}{}^{\text{CP}}\text{G}$ . For both bridge lengths, the quantum yield of  ${}^{\text{CP}}\text{G}$  decomposition when incoherent transport is blocked is similar to the quantum yield of emission quenching by guanine. This is consistent with our assignment of the emission quenching yield as the yield of coherent CT to guanine.

There is evidence for delocalization from the yield of  ${}^{\text{CP}}\text{A}$  decomposition. Significantly less  ${}^{\text{CP}}\text{A}$  decomposition is observed for  $\text{Ap-A}_5\text{-}{}^{\text{CP}}\text{A}^3\text{-}{}^{\text{CP}}\text{G}$  than for  $\text{Ap-A}_6\text{-}{}^{\text{CP}}\text{A}^3\text{-}{}^{\text{CP}}\text{G}$ , where the only difference is the number of adenines between  ${}^{\text{CP}}\text{A}$  and

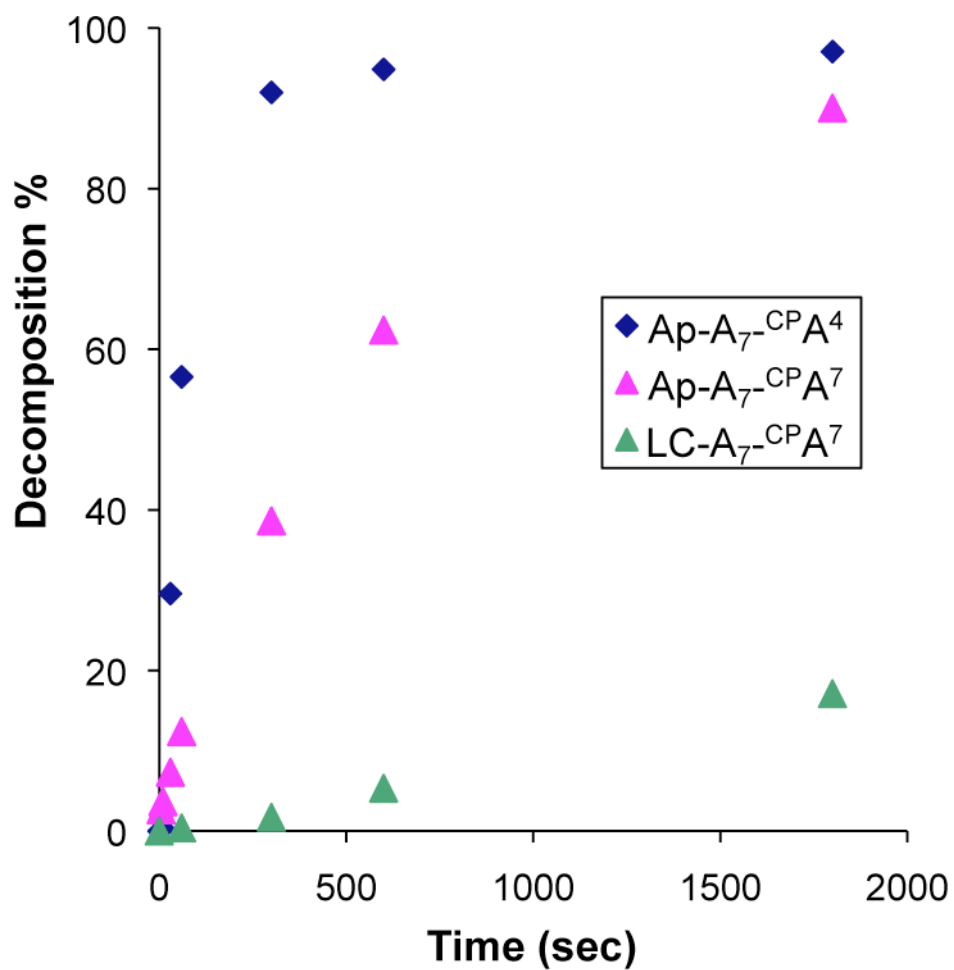


**Figure 3.5.** Time courses of <sup>CP</sup>A decomposition by irradiation of Ap-A<sub>7</sub>-CPA<sup>4</sup> (blue diamonds), Ap-A<sub>7</sub>-CPA<sup>7</sup> (purple triangles), and LC-A<sub>7</sub>-CPA<sup>7</sup> (green triangles). The decomposition in each case follows first-order kinetics. 10 μM duplexes were irradiated at 325 nm. Conditions are as provided in Methods.

$^{\text{CP}}\text{G}$ . For two, but not three intervening adenines,  $^{\text{CP}}\text{G}$  is competent to compete with  $^{\text{CP}}\text{A}$  for the radical. This sensitivity to a distal trap could be due to polaron formation or transient delocalization along the adenine tract. We have previously observed similar behavior for oxidation of the higher-potential  $^{\text{CP}}\text{C}$  near  $^{\text{CP}}\text{G}$ , although in that case competition was not apparent for more than a single intervening adenine.<sup>17</sup>

Intriguingly,  $^{\text{CP}}\text{A}$  decomposition is insensitive to whether the distant base is an inosine or guanine. When there is no guanine at the end of the adenine tract, the coherent CT pathway that leads to fluorescence quenching is eliminated. If coherent and incoherent CT are in competition, this should lead to an increase in the yield of charge injection to the adenine tract, but such increase in injection is not observed. Hence, incoherent and coherent CT must be proceeding from different populations, as in

### **Figure 3.2.**

We also observe sensitivity to the length of the adenine tract; Ap-A<sub>5</sub>- $^{\text{CP}}\text{A}^4$  and Ap-A<sub>7</sub>- $^{\text{CP}}\text{A}^4$  differ only in the length of the adenine tract, yet the quantum yield of  $^{\text{CP}}\text{A}$  decomposition increases by 50% for the latter assembly. The longer adenine tract has more runs of 3–4 AT base pairs that include the  $^{\text{CP}}\text{A}$ , and hence can accommodate more low-potential delocalized orbitals. Again, both a self-trapped polaron following injection and transient delocalization prior to injection are consistent with this interpretation.

### **3.4. CONCLUSIONS**

We have performed direct comparison of the absolute yields of coherent and incoherent CT in the same DNA assemblies, demonstrating that coherent CT dominates the incoherent channel at a donor-bridge separation of 2.7 nm, but not for shorter adenine

tracts. The change of mechanism could not be determined from analyzing only the distance dependence of the total yield, which is fit equally well by exponential (superexchange) and geometric (hopping) decays. The transition from multi-step to single-step transport, opposite to that typically found across molecular bridges, is due to a shallower distance dependence for coherent CT versus incoherent hopping. The steeper decay for hopping might be due to coulomb attraction within the radical ion pair intermediate, while the shallow decay of coherent CT indicates that the distance dependence does not reflect the drop in bridge-mediated electronic coupling, but rather represents the conformational dynamics for forming a CT-active state. Coherent and incoherent CT do not appear to be in competition, implying that CT-active states favor the former and CT-inactive states favor the latter.

Over a long adenine tract that can accommodate delocalized domains, long-distance single-step CT dominates the overall transport. Models of DNA-mediated CT must consider the contribution of long-range transfer, subject to sequence-dependent conformational dynamics.

**3.5. REFERENCES:**

- 1) Chen, F.; Hihath, J.; Huang, Z.; Li, X.; Tao, N.J. *Annu. Rev. Phys. Chem.* **2007**, *58*, 535.
- 2) Davis, W.B.; Ratner, M.A.; Wasielewski, M.R. *J. Am. Chem. Soc.* **2001**, *123*, 7877.
- 3) Weiss, E.A.; Ratner, M.A.; Wasielewski, M.R. *Top. Curr. Chem.* **2005**, *257*, 103.
- 4) Newton, M.D.; Smalley, J.F. *Phys. Chem. Chem. Phys.* **2007**, *9*, 555.
- 5) Berlin, Y.A.; Grozema, F.C.; Siebbeles, L.D.A.; Ratner, M.A. *J. Phys. Chem. C* **2008**, *112*, 10988.
- 6) Weiss, E.A.; Tauber, M.H.; Kelley, R.J.; Ahrens, M.J.; Ratner, M.A.; Wasielewski, M.R. *J. Am. Chem. Soc.* **2005**, *127*, 11842.
- 7) Goldsmith, R.H.; Sinks, L.E.; Kelley, R.F.; Betzen, L.J.; Liu, W.; Weiss, E.A.; Ratner, M.A.; Wasielewski, M.R. *Proc. Natl. Acad. Sci. U.S.A.* **2005**, *102*, 3540.
- 8) Murphy, C.J.; Arkin, M.R.; Jenkins, Y.; Ghatlia, N.D.; Bossmann, S.H.; Turro, N.J.; Barton, J.K. *Science* **1993**, *262*, 1025.
- 9) Lewis, F.D.; Liu, J.; Weigle, W.; Rettig, W.; Kurnikov, I.V.; Beratan, D.N. *Proc. Natl. Acad. Sci. U.S.A.* **2002**, *99*, 12536.
- 10) Drummond, T.G.; Hill, M.G.; Barton, J.K. *Nat. Biotechnol.* **2003**, *21*, 1192.
- 11) Takada, T.; Fujitsuka, M.; Majima, T. *Proc. Natl. Acad. Sci. U.S.A.* **2007**, *104*, 11179.
- 12) Merino, E.J.; Boal, A.K.; Barton, J.K. *Curr. Op. Chem. Biol.* **2008**, *12*, 229.
- 13) Genereux, J.C.; Barton, J.K. *Chem. Rev.* **2009**, *in press*.
- 14) O'Neill, M. A.; Barton, J. K. *J. Am. Chem. Soc.* **2004**, *126*, 11471.

- 15) Adhikary, A.; Kumar, A.; Khanduri, D.; Sevilla, M.D. *J. Am. Chem. Soc.* **2008**, *130*, 10282.
- 16) Conwell, E. M.; Bloch, S. M. *J. Phys Chem. B* **2006**, *110*, 5801.
- 17) Shao, F.; Augustyn, K. E.; Barton, J. K. *J. Am. Chem. Soc.* **2005**, *127*, 17445.
- 18) O'Neill, M. A.; Barton, J. K. *J. Am. Chem. Soc.* **2004**, *126*, 13234.
- 19) Genereux, J.C.; Augustyn, K.E.; Davis, M.L.; Shao, F.; Barton, J.K. *J. Am. Chem. Soc.* **2008**, *130*, 15150.
- 20) Hall, D.B.; Holmlin, R.E.; Barton, J.K. *Nature* **1996**, *382*, 731.
- 21) Liu, C.-S.; Hernandez, R.; Schuster, G.B. *J. Am. Chem. Soc.* **2004**, *126*, 2877.
- 22) Williams, T. T.; Dohno, C.; Stemp, E. D. A.; Barton, J. K. *J. Am. Chem. Soc.* **2004**, *126*, 8148-8158.
- 23) Shafirovich, V.; Dourandin, A.; Huang, W.; Geacintov, N.E. *J. Biol. Chem.* **2001**, *276*, 24621.
- 24) Nakatani, K.; Dohno, C.; Saito, I. *J. Am. Chem. Soc.* **2001**, *123*, 9681.
- 25) O'Neill, M. A.; Dohno, C.; Barton, J. K. *J. Am. Chem. Soc.* **2004**, *126*, 1316.
- 26) Augustyn, K. E.; Genereux, J. C.; Barton, J. K. *Angew. Chem. Int. Ed.* **2007**, *46*, 5731.
- 27) Hatchard, C. G.; Parker, C. A. *Proc. R. Soc. Lon. Ser. A* **1956**, *235*, 518.
- 28) O'Neill, M.A.; Barton, J.K. *Proc. Natl. Acad. Sci. U.S.A.* **2002**, *99*, 16543.
- 29) Kelley, S. O.; Barton, J. K. *Science* **1999**, *283*, 375.
- 30) Somsen, O.J.G.; Keukens, L.B.; de Keijzer, M.N.; van Hoek, A.; van Amerongen, H. *ChemPhysChem* **2005**, *6*, 1622.
- 31) Manoj, P.; Min, C.-K.; Aravindakumar, C.T.; Joo, T. *Chem. Phys.* **2008**, *352*, 333.

- 32) Wan, C.; Fiebig, T.; Schiemann, O.; Barton, J.K.; Zewail, A.H. *Proc. Natl. Acad. Sci. U.S.A.* **2000**, *97*, 14052.
- 33) Fiebig, T.; Wan, C.; Zewail, A.H. *ChemPhysChem* **2002**, *3*, 781.
- 34) Wan, C.; Xia, T.; Becker, H.-C.; Zewail, A.H. *Chem. Phys. Lett.* **2005**, *412*, 158.
- 35) Hardman, S.J.O.; Thompson, K.C. *Biochemistry* **2006**, *45*, 9145.
- 36) Perun, S.; Sobolewski, A.L.; Domcke, W. *Mol. Phys.* **2006**, *104*, 1113.
- 37) O'Neill, M. A.; Becker, H. C.; Wan, C.; Barton, J. K.; Zewail, A. H., *Angew. Chem. Int. Ed.* **2003**, *42*, 5896-5900.
- 38) Goldsmith, R.H.; DeLeon, O.; Wilson, T.M.; Finklestein-Shapiro, D.; Ratner, M.A.; Wasielewski, M.R. *J. Phys. Chem. A* **2008**, *112*, 4410.
- 39) Lewis, F.D.; Zhu, H.; Daublain, P.; Cohen, B.; Wasielewski, M.R. *Angew. Chem. Int. Ed.* **2006**, *45*, 7982.
- 40) Jortner, J; Bixon, M.; Langenbacher, T.; Michel-Beyerle, M.E. *Proc. Natl. Acad. Sci. USA* **1998**, *95*, 12759.
- 41) Grozema, F.C.; Tonzani, S.; Berlin, Y.A.; Schatz, G.C.; Siebbeles, L.D.A.; Ratner, M.A. *J. Am. Chem. Soc.* **2008**, *130*, 5157.